AD-A148 662 A SPECTROELECTROCHEMICAL INVESTIGATION OXIDATION OF THE BILIRUBIN IX-ALPA..(U) UTAH UNIV SALT LAKE CITY DEPT OF CHEMISTRY J R PRADKO ET AL. 28 NOV 84 TR-32 1/1

UNCLASSIFIED N00014-83-K-0470 F/G 6/1 NL

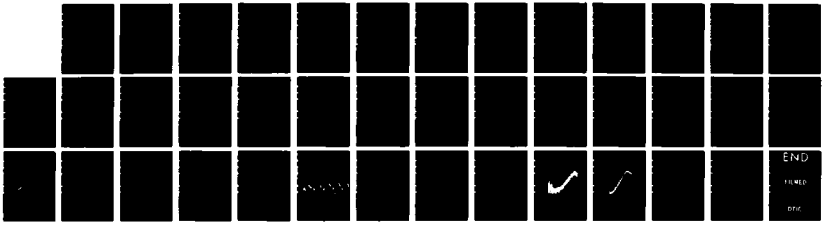

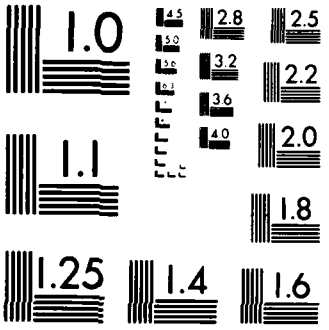

OFFICE OF NAVAL RESEARCH

Contract N00014-83-K-0470

Task No. NR 359-718

TECHNICAL REPORT NO. 32

A Spectroelectrochemical Investigation Oxidation of the Bilirubin IX-α in Dimethylformamide

By

John R. Pradko
Stanley Pons
Jerome F. McAleer
A. Scott Hinman

Prepared for Publication in

J. Bioelectrochem. and Bioenerg.

University of Utah
Department of Chemistry
Salt Lake City, Utah 84112

November 28, 1984

SECURITY CLASSIFICATION OF THIS PAGE (When Data Entered)

REPORT DOCUMENTATION PAGE

READ INSTRUCTIONS BEFORE COMPLETING FORM

1. REPORT NUMBER: 32	2. GOVT ACCESSION NO.: AD-A148662
3. RECIPIENT'S CATALOG NUMBER:	
4. TITLE (and Subtitle): A Spectroelectrochemical Investigation Oxidation of the Bilirubin IX-α in Dimethylformamide	5. TYPE OF REPORT & PERIOD COVERED: Technical Report # 32
	6. PERFORMING ORG. REPORT NUMBER:
7. AUTHOR(s): John R. Pradko; Stanley Pons*; Jerome F. McAleer; A. Scott Hinman	8. CONTRACT OR GRANT NUMBER(s): N00014-83-K-0470
9. PERFORMING ORGANIZATION NAME AND ADDRESS: University of Utah, Department of Chemistry, Salt Lake City, UT 84112	10. PROGRAM ELEMENT, PROJECT, TASK AREA & WORK UNIT NUMBERS: Task No. NR 359-718
11. CONTROLLING OFFICE NAME AND ADDRESS: Office of Naval Research, Chemistry Program - Chemistry Code 472, Arlington, Virginia 22217	12. REPORT DATE: November 28, 1984
	13. NUMBER OF PAGES: 37
14. MONITORING AGENCY NAME & ADDRESS (if different from Controlling Office)	15. SECURITY CLASS. (of this report): Unclassified
	15a. DECLASSIFICATION/DOWNGRADING SCHEDULE

16. DISTRIBUTION STATEMENT (of this Report)

This document has been approved for public release and sale; its distribution unlimited.

17. DISTRIBUTION STATEMENT (of the abstract entered in Block 20, if different from Report)

18. SUPPLEMENTARY NOTES

19. KEY WORDS (Continue on reverse side if necessary and identify by block number)

Spectroelectrochemistry, Bilirubin

20. ABSTRACT (Continue on reverse side if necessary and identify by block number)

The electrochemistry of bilirubin IX-α in N,N-dimethylformamide has been investigated by cyclic voltammetry, ac voltammetry, modulated specular reflectance spectroscopy, small amplitude ac reflectance spectroscopy, OTTLE cell spectroelectrochemistry, and conventional spectroscopy. The data suggest a CECEC mechanism for oxidation of bilirubin to biliverdin. The oxidation potential for the mono-deprotonated bilirubin to its cation radical is +0.10 V, and for the carbonium ion/free radical couple, -0.86 V vs Ag/Ag^+ (0.10 M).

DD FORM 1 JAN 73 1473 EDITION OF 1 NOV 65 IS OBSOLETE

S/N 0102-LF-014-6601

Unclassified

SECURITY CLASSIFICATION OF THIS PAGE (When Data Entered)

A Spectroelectrochemical Investigation

Oxidation of the Bilirubin IX-α in Dimethylformamide

John R. Pradko
The Medical School
University of Iowa
Des Moines, Iowa
U.S.A.

Stanley Pons*
Department of Chemistry
University of Utah
Salt Lake City, UT 84112
U.S.A.

Jerome F. McAleer
Department of Chemistry
The University
Southampton, Hants. SO9 5NH
ENGLAND

A. Scott Hinman
Department of Chemistry
University of Calgary
Calgary, Alberta
CANADA

*To whom all correspondence should be addressed.

Abstract

The electrochemistry of bilirubin IX-α in N,N-dimethylformamide has been investigated by cyclic voltammetry, ac voltammetry, modulated specular reflectance spectroscopy, small amplitude ac reflectance spectroscopy, OTTLE cell spectroelectrochemistry, and conventional spectroscopy. The data suggest a CECEC mechanism for oxidation of bilirubin to biliverdin. The oxidation potential for the mono-deprotonated bilirubin to its cation radical is +0.10 V, and for the carbonium ion/free radical couple, -0.86 V vs Ag/Ag^{+} (0.10 M).

Introduction

Bilirubin IX-α (Br, Figure 1) is an open-chained tetropyrrole formed in the body from the enzymatic reduction of biliverdin IX-α (Bv, Figure 1) which is a product resulting from the catabolism of heme. Bilirubin normally is converted to a water soluble diglucuronide in the liver (Figure 1) and excreted via the bile into the duodenum where it is further converted by the bacterial flora to final products: urobilinogen, stercobilinogen, urobilin, and stercobilin. Under some conditions, especially in infants where the lifetime of a red blood cell is quite short, an excessive amount of bilirubin may be formed leading to jaundice or the sometimes fatal condition known as kernicterus.

There are a variety of oxidation reactions known for bilirubin. One of these, photo-oxidation at near-UV wavelengths, is the clinically accepted method for reducing serum bilirubin levels in jaundiced infants. In general, mechanistic details for these oxidative pathways are not well understood. It is the purpose of this paper to report the details of the mechanism of the electrochemical oxidation of bilirubin in an aprotic solvent to provide information that may be of value in the understanding of the naturally occurring processes. The work will also demonstrate the application of new spectroelectrochemical techniques which promise to be of value in complicated reaction analyses.

Spectroscopic Techniques

Modulated specular reflectance spectrscopy (MSRS, (1, 2)), was performed by measuring the normalized difference in reflection ($\Delta R/R = R_2-R_1/R_1$; R_1 = reflectance at base potential E_1, R_2 = reflectance at working potential E_2) at a platinum mirror electrode as a function of wavelength. The measured value of $\Delta R/R$ at a specific wavelength as a function of time is given explicitly by:

$$\ln\left(\frac{\Delta R}{R} + 1\right) = \frac{-4.606\ \Delta\varepsilon}{nFA\cos\theta}\left[\int (i(t)dt + K(t))\right] \qquad [1]$$

where $\Delta\varepsilon$ is the difference in molar absorbtivity of the chromophores present at E_1 and E_2, θ is the angle of incidence of radiation at the electrode, i(t) is the current contributing to the conversion of the chromophore(s), K(t) contains homogeneous reaction rate expressions involving the chromophore(s), and n, F, and t have their usual significance. The theory, cell design, and experimental implementation of the technique has been described in detail (3). Spectra recorded by the technique represent both species formed during an electrochemical reaction, and species removed from the diffusion layer during the same process. Absorbance-time transients may then be recorded by the same technique at appropriate wavelengths, the shape of which are governed by equation [1]. The kinetic parameters of the total electrochemical reaction, which are in the i(t) and K(t) terms, may thus be determined by analysis of the $\Delta R/R$-t curves. The most important advantage of the analysis is molecular specificity, and the lack of interferences from other electrode processes which always contribute to the measured current $i(t)_m$ in a conventional dc electrochemical experiment (capacitive charging, non-absorbing electroactive impurities, etc.).

An immediate extension to this technique is the ac equivalent: sinusoidally modulated ac reflectance spectroscopy (SMACRS, (4)). If a small amplitude sinusoidal perturbation is superimposed on a slowly varying cyclic potential ramp, the resulting ac reflectance response corresponding to the fundamental harmonic component of the applied modulation frequency, is given,

for a simple reversible redox reaction, by

$$R(\omega t) = \frac{4.606\ \Delta\varepsilon}{\omega n\ F\ \cos\ \theta}\ I_{REV}\ F(t)G(\omega)\ \cos(\omega t + \phi) \qquad [2]$$

where I_{REV} is the fundamental harmonic faradaic component of the current, F(t) and G(ω) are functions which describe the effects of non-nernstian behavior of the response on the dc and ac timescales respectively, ω is the angular frequency of modulation and Ø is the phase angle between the current and applied potential (5). We have shown that the spectrophotometric response is simply proportional to the current response, so that those well known current equations may be used to describe the system, in our case, however, without having to be concerned with capacitive charging effects (4).

Experimental

Chemicals 99.9% bilirubin was prepared by a procedure similar to that described by Fog (6). Commercial reagent grade bilirubin contains several of the bilirubin isomers, usually created during isolation and purification of the IX-α natural isomer. The commercial material, generally isolated from oxen bile or gallstones, was dissolved in chloroform by boiling for a few seconds. The solution was filtered, and cooled to room temperature. The filtrate was chromatographed on a column of pure, anhydrous sodium sulfate which retained biliverdin and mono- and dipyrrole impurities. Photochemical degradation was prevented by wrapping the column with aluminum foil. The eluent was reduced in volume 40% by distillation. The hot solution was filtered on a hot water funnel, and cooled to -20°C for 24 h. Most of the

bilirubin remaining dissolved was precipitated by adding an equal volume of cooled diethyl ether to the solution. The entire precipitate was collected and washed with cold diethyl ether until the ether was colorless. The product was dried in vacuo at room temperature in the dark for 24 h. The yield based on the amount of starting material was 55%. Remaining impurities could not be detected by conventional spectroscopy or voltammetry.

Biliverdin of similar purity was prepared by a procedure similar to Manitto and Monti (7). 300 mg bilirubin purified as described above was added to 400 mg tetrachloro-1,4-benzoquinone(chloronil) and 570 mg picric acid in 20 mL t-butanol. The mixture was dissolved in 500 mL chloroform (ethanol free) and purged with argon for 15 m. The flask was sealed from the atmosphere and stored in the dark for 8 d. As oxidation progresses, the solution changes from orange to dark green. The chloroform was evaporated on a rotary evaporator, and 100 mL 5:100::methanol:benzene v/v was added to the precipitate. After stirring vigorously, the green biliverdin-picric acid complex was collected by filtration and washed with benzene. The complex was dissolved in 4 mL dimethylsulfoxide and added to 300 mL ethyl acetate with stirring. The solution was washed in a separatory funnel with 50 mL aliquots of distilled water until the water phase was colorless (~ 10 aliquots). The biliverdin was filtered from the ethyl acetate solution and dried in vacuo at room temperature for 24 h. The yield was ~ 50 mg. TLC on silica gel (5:100::methanol:benzene v/v, 24°C) gives a single spot with R_f = 0.23. The UV/VIS adsorption spectrum has maxima at 384 and 650 nm in dimethylforamide solution.

Tetra-n-butylammonium tetrafluoroborate was prepared according to the method of Lund and Iversen (8).

Instrumentation:

Electrochemical measurements were performed with a Hi-Tek DT2101 potentiostat driven by a Hi-Tek PPR1 waveform generator. A Bentham lock-in amplifier was used for the spectroelectrochemical measurements requiring synchronous demodulation. Slow responses were recorded on a Hewlett-Packard X-Y recorder, while fast responses were recorded on a Hi-Tek AA1-512 digital signal averager. The experimental arrangement for modulated specular reflectance spectroscopy (MSRS) and sinusoidally modulated ac reflectance spectroscopy (SMACRS) has been described in a previous report (4).

The optical cell used for MSRS and SMACRS was of the conventional 45° reflectance type (3), and the thin layer cell was constructed from two quartz plates fused together and containing a 0.2 mm thick x 30 mm long x 5 mm wide platinum gauze working electrode, two 0.2 mm diameter Pt wires oriented parallel to the length of the working electrode on each side serving as secondary electrodes, and 2 thin pieces of filter paper separating the working electrode from the secondaries. The paper served to slow diffusion between the electrodes. The parallel arrangement of electrodes facilitated a uniform potential distribution across the length of the gauze so that rapid generation of chromophore in the total interstitial space of the gauze was afforded. Electrolysis was several times more rapid than that in conventional OTTLE cells having the secondary electrode external to the "sandwich". This is especially important in systems such as those described herein in which the specific resistivity of the electrolyte is high (9).

Results

D.C. Voltammetry

All cyclic voltammetric experiments were performed on solutions prepared from 0.15 M tetra-n-butylammonium tetrafluoroborate in dimethylformamide. Potentials reported are with respect to a 0.10 M Ag^+/Ag reference electrode in the same electrolyte. Solutions were saturated with dry argon before measurement.

The voltammetry of a 0.50 mM solution of bilirubin is shown in Figure 2. The potential sweep rate ν was 0.100 Vs^{-1}. For a positive potential sweep beginning at -0.40 V and reversing at +0.60 V there are three prominent oxidation peaks: +0.10, +0.24, and +0.47 V. If the solvent is not completely free from basic impurities (see below) there is another oxidation wave at -0.21 V (dotted curve in Figure 2). A negative sweep beginning at 0.0 V and reversing at -2.30 V has one reduction peak at -1.55 V and an oxidation peak on the reverse positive sweep at -1.00 V.

Figure 3 shows the result under the same conditions if the potential sweep is initiated (3A) in the positive direction first and then swept to include the reductions, and (3B) in the negative direction first and then cycled to include the first oxidation peak. In (3A), two new reduction peaks at -0.88 and -1.35 are observed. In (3B) it is evident that these two processes are related to species formed in the oxidation process at +0.10 V.

Figures 4 and 5 show the cyclic voltammograms for 0.50 mM biliverdin under the same conditions as described for bilirubin. Figure 4A shows two oxidations at +0.24 and +0.47 V as does bilirubin. The negative sweep shows two reduction processes at -1.35 and -1.55 V (Figure 4B). There is an accompanying oxidation at -1.00 V. Figure 4C shows the voltammetry for biliverdin hydrochloride. In this case, a new reduction wave appears at -0.88

V, and the -1.35 and -1.55 V peaks coalesce into a broad reduction wave. The corresponding dependence of the voltammetry on the initial sweep direction is shown in Figure 5. It is noted that the -0.88 V reduction wave only appears if the wave at +0.24 V is included in the program.

Figure 6 shows the behavior of the oxidation peaks when base (tetrabutylammonium hydroxide) is added to the bilirubin solution. The aforementioned oxidation peak at -0.21 increases quantitatively with base concentration, and the oxidation peak at +0.10 V decreases in intensity. The oxidation wave at +0.24 V was unaffected by base.

The effect on the first oxidation wave at +0.10 V for bilirubin of addition of trifluoroacetic acid is shown in Figure 7 as a function of potential sweep rate. The slopes of the plots decrease as acid is added.

Figure 8 shows the repetitive cyclic voltammetry of bilirubin between -1.20 V and +0.14 V at a sweep rate of 0.15 Vs^{-1}. Upon continued cycling, three points are noted: (1) The oxidation at +0.10 V decreases only slightly before reaching an equilibrium value. (2) After the first excursion to the peak at +0.10 V, the peak at -.88 V begins to increase, and on continued cycling builds to an equilibrium value. (3) A new oxidation wave at -0.82 V appears and also approaches an equilibrium value on continued cycling. This wave was present in neutral and basic solutions, but disappeared on the addition of acid to the solution. This couple disappears if the potential sweep is truncated so as not to include the peak at +0.10 V. The continued cycling about the +0.10 V peak but excluding the -0.88/-0.82 couple results in rapid diminuation of the height of the +0.10 V peak.

A.C. Voltammetry

The ac voltammetry of a 0.50 mM solution of bilirubin is shown in Figure 9 as a function of modulation frequency. The height of the +0.24 V dc peak

increased with frequency as expected, while the first oxidation peak decreased with increasing frequency. The dc sweep rate ν was 0.005 Vs^{-1}, and the modulation amplitude was 0.0035 V_{RMS}. The $i(\omega t)$ reported is the value of the component of the current in phase with the applied potential.

UV-VIS Spectra

The electronic spectra of bilirubin and some of its oxidation products formed in the described modified OTTLE cell are shown in Figure 10. The bilirubin substrate spectrum is shown in Figure 10A. After 30 s electrolysis at +0.12 V (Figure 10B), peaks at 384 and 670 nm are prominent and the bilirubin peak at 453 nm is decreasing in intensity. In 4 m, all of the bilirubin has been oxidized to biliverdin. At +0.25 V (Figure 10C), peaks at 336 and 550 nm (purpurin) replace those produced at +0.12 V, and at +0.51 V (Figure 10D) peaks at 312 and 487 nm (choletellin) replace those formed at +0.25 V.

If 0.50 mM trifluoroacetic acid is added to the biliverdin solution in the spectrometer, the peak at 650 nm shifts to 670 nm.

SMACRS Spectra

The ac reflectance responses, $R(\omega t)$ for a linear potential sweep through the first two bilirubin oxidation peaks are shown in Figure 11 as a function of wavelength. The dc potential sweep rate was 0.005 Vs^{-1}, and the modulation was 0.030 V p-p at 45 Hz. The bipolar response indicates first the appearance of a bilirubin oxidation product [negative values of $R(\omega t)$] followed by the removal of an absorbing species from the diffusion layer at higher positive potentials [positive values of $R(\omega t)$]. A plot of the two $R(\omega t)$ maxima (+0.04 V and +0.15 V) as a function of wavelength of radiation is shown in Figure 12.

Figures 13 and 14 show the SMACRS response and corresponding voltammetry for a 0.50 mM bilirubin solution at 546 nm from 0.0 to +0.50 V as a function

of added acid (trichloroacetic) and added base (tetra-n-butylammonium hydroxide) respectively. The magnitude of the reflectance response is seen to decrease markedly with increasing base strength, as does the intensity of the first voltammetric wave.

In acid solution (Figure 14), there is a shift of both voltammetric peaks to more positive potentials. $R(\omega t)$, associated with the second oxidation peak, exhibited a maximum negative value at 0.28 mM acid concentration. Further addition of acid resulted in a diminished reflectance response.

MSRS Response

The modulated specular reflectance spectrum for a 0.5 mM bilirubin solution between the potential limits of -0.50 and +0.20 V is shown in Figure 15. The weak signal $[(\Delta R/R)_{MAX} = 8 \times 10^{-5}]$ has a maximum absorbance at 675 nm and corresponds to absorption of a species being formed at the more positive potential. The shape of the band at slightly shorter wavelengths suggests that another band may be present. The modulation frequency was 40 Hz.

If the potential limits are increased to -1.20 and +0.20 V to include the first redox couple at negative potentials, a much stronger MSRS signal $[(\Delta R/R)_{MAX} = 1 \times 10^{3}]$ is evident (Figure 16). There are two distinct bands at 636 and 675 nm, with the 636 nm band being stronger in intensity. If the modulation frequency is increased to 80 Hz, the 675 nm band is greatly attenuated with respect to the 636 nm band. The downward (positive) value of $\Delta R/R$ below 560 nm represents the consumption (loss of absorption) of bilirubin in the diffusion layer.

Figure 17 shows $\Delta R/R$-time transients recorded at 636, 625, and 675 nm respectively. The base potential was -1.20 V and the upper potential (rising portion of transient) was +0.20 V. The electrode pulsed to +0.20 V for 100 ms and allowed to recover for 10 s; $\Delta R/R$ was signal averaged for 64 scans to increase S/N.

DISCUSSION

The first voltammetric oxidation peak for bilirubin in DMF at +0.10 V has been identified previously (10) as the two election process leading to production of biliverdin. The process at +0.24 V, as evidenced by (a) the spectroscopy of the solution obtained after electrolysis and (b) the similarity in the voltammetry of pure biliverdin, is the two election oxidation of biliverdin to purpurin. The same experiment on purpurin solutions leads to our attributing the peak at +0.47 V to the two election oxidation of purpurin to choletellin. (see Figure 18).

The data in Figure 8 suggest that the bilirubin substrate is regenerated if the voltammetric sweep range is -1.20 to + 0.20 V. The reduction wave at -0.88 V appears only if oxidation at 0.10 V has occurred, and is thus the reduction of an oxidation product or intermediate formed at +0.10 V. The oxidation at -0.82 V appears only after the reduction at -0.88 V. This couple obeys the criteria defined for a simple reversible one election redox reaction. If the negative sweep limit is made more positive, the rapid decrease in the peak height of the oxidation at +0.10 V indicates that bilirubin was being regenerated from a homogeneous chemical reaction following the oxidation reaction at -0.82 V, or that bilirubin itself is the direct product of the election transfer at that potential. The possibility that the wave at -0.88 V is the reduction of protons generated after electron transfer at +0.10 V was eliminated by performing the same experiment at a vitreous carbon electrode. The peak remained, and is therefore not due to proton reduction (proton reduction is shifted to more negative potentials on vitreous carbon).

The height of the biliverdin oxidation peak at +0.24 V decreases relative to the bilirubin peak (+0.10 V) with increasing potential sweep rate, leading

to the conclusion that at least one of the deprotonation steps in the bilirubin oxidation is slow. Since at sweep speeds up to 150 Vs^{-1} there is no reverse wave observed corresponding to the +0.10 V peak, and since there is never any indication of a transition region for n = 2 to n = 1 in the $i_p - \nu^{1/2}$ plots of the voltammetric data, then it may also be concluded that either an ee step is involved, or if a deprotonation step occurs in an ece sequence, the deprotonation is very fast.

The reduction waves at -1.35 and -1.55 V are the reductions of biliverdn and bilirubin respectively, as determined from the voltammetry of the pure compounds, and the bilirubin behavior at those potentials after initial bilirubin oxidation.

The oxidation wave at -1.00 V is associated with products formed from bilirubin reduction at -1.55 V, and the oxidation wave at -0.21 V has been previously reported (10) as the oxidation of the dianion of bilirubin, and is supported in this work: addition of base (Figure 6) apparently quantitatively converts bilirubin to the species oxidized at -0.21 V. It was also observed that this wave could only be totally eliminated if the dimethylformamide solvent used was very pure. Basic degradation products (amines), present within 24 hours after distillation and storage in the dark, were sufficient to cause the wave to appear.

The decrease in slope of the $i_p - \nu^{1/2}$ plots and an anodic shift for the +0.10 V wave with increased acid strength of the solution indicates that there is a deprotonation step between the two electron transfers, and that it is reversible. The subsequent oxidation peak at +0.24 V, the oxidation of biliverdin, decreases with increased potential scan rate indicating a final homogeneous chemical step (the second deprotonation) after the two election oxidation of the bilirubin. The possibility of a slow second election

transfer is discounted since an n = 2 to 1 transition is not observed at high voltammetric sweep rates. The appearance of the -0.88/-0.82 V couple supports a mechanism of two electron transfers with $E_2 < E_1$. An EEC type mechanism, with both electron transfers occurring at the same potential (11, 12) must thus be discounted as a possibility. In a simplified "scheme of squares" [3] for two election transfers and two proton losses, we suggest the ECEC path (circled) as the most likely path for the first voltammetric wave oxidation: (Br = bilirubin; Bv = Biliverdin)

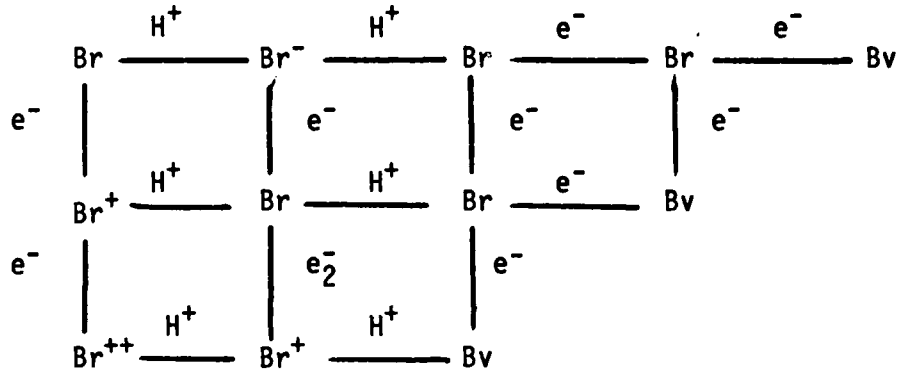

Since the last proton loss is slow, it is reasonable to assign the -0.88/-0.82 V reversible couple to the $Br^+ + e_2^- \rightleftarrows Br^{\cdot}$ reaction. It is thus the relatively stable Br^+ species that is responsible for the 636 nm adsorption maximum.

The behavior of the adsorbance-time transients of Figure 17 are now readily explained in terms of this proposed mechanism. Pulsing the electrode from -1.20 V to +0.20 V for 100 ms produces ultimately Br^+ with λ_{max} = 636 nm. It is pointed out that the transient of maximum intensity is observed at this wavelength. The rate of rise of this transient, if it were for a simple reversible redox process, should be proportional to $t^{1/2}$. With the following deprotonation reaction:

$$Br^+ - H^+ \longrightarrow Bv \qquad [4]$$

$$Bv + H^+ \xrightarrow{fast} \text{protonated Bv } (\lambda_{max} = 675 \text{ nm})$$

considered, a plot of $\frac{\Delta R}{R}$ vs $t^{1/2}$ should be sublinear (2). The observed result, however, is that the $\frac{\Delta R}{R}$ vs $t^{1/2}$ plot is superlinear, a result expected if protonated Bv is a stronger absorber (λ_{max} = 675 mm) at 636 nm than the Br^+. In fact, the rate constant for the deprotonation reaction [4] is given by (15):

$$k = \frac{[\frac{\Delta R}{R}]_k^T (t) - [\frac{\Delta R}{R}]_o^{Br^+}(t)}{\int (1 + \frac{\Delta\epsilon}{\epsilon_{Br^+}})[\frac{\Delta R}{R}]_o^{Br+}(t) - [\frac{\Delta R}{R}]_k^T(t)\ dt} \qquad [5]$$

where $[\frac{\Delta R}{R}]_k^T$ (t) is the total observed normalized difference reflectance response as a function of time (for Br^+ and Bv), $[\frac{\Delta R}{R}]_o^{Br+}$ is the corresponding value for Br^+ in the absence of the final kinetic step, and $\Delta\epsilon = \epsilon_{Bv} - \epsilon_{Br^+}$ where ϵ_{Bv} and ϵ_{Br^+} are the molar extinction coefficients for protonated Bv and Br^+ respectively. Since Br^+ is produced first in the overall reaction scheme, the value of $[\frac{\Delta R}{R}]_o^{Br+}$ (t) is simply the linear extrapolation of the $[\frac{\Delta R}{R}]_k^T$ (t) vs $t^{1/2}$ plot at short times. The rate constant k is thus obtained from graphical integration (see reference 2) and was found to be 0.61 ± 0.2 s^{-1}. When the pulse to +0.20 V was terminated (100 ms after initiation) the $\frac{\Delta R}{R}$ response was observed to fall at a rate much slower than that expected from a simple single chromophere redox process, but again was predictable in terms of the process just described. The complete description

of the expected response is the subject of a forthcoming report (15).

The voltammetry in dimethylformamide, however, appears to be incomplete. It is well known that there are two weak acid protons in the molecule, and they both have been shown to be titrated with tetramethylguanidine (13). Electrochemically, however, there are only two oxidation waves: 0.10 V (previously assigned as the neutral species) and -0.21 V (dianion). It is likely that the bilirubin molecule does not exist in dimethylformamide as the neutral species, but the monoanion. The electroactive species, in the presence of any base, are then related by the equilibrium:

$$\underset{(E_{ox} = 0.10\ V)}{Br^-} + \text{base} \rightleftharpoons \underset{(E_{ox} = -0.21\ V)}{Br^=} \qquad [6]$$

The <u>in situ</u> spectrophotometric results support this possibility, and give additional insight into the overall process. The composite SMACRS spectrum (Figure 12) indicates that at 670 nm the observed species being removed from the solution at 0.15 V is protonated biliverdin as might be suspected: the strong acidic conditions in the diffusion layer due to loss of 2 protons from bilirubin is certainly sufficient to protonate biliverdin. Protonated biliverdin is apparently the final oxidation product. Exhaustive electrolysis of bilirubin in the first wave (+0.10 V) also gives the 670 nm maximum instead of the 650 nm maximum (as does the acidic biliverdin hydrochloride) observed when pure neutral biliverdin is prepared independently as described in the experimental section.

The pH dependence of the first oxidation wave (Figure 7) as well as the results of Koch and Akingbe (14), showing similar results, support Br^- being

the electroactive species. Ultimately, the electron transfers and proton loss reactions occur at the center pyrrole nitrogen (Figure 18). In the neutral species, the two carboxylic acid groups are hydrogen bonded to these pyrrole nitrogens causing distortion of the molecule (13) and inhibition of charge transfer. Loss of the carboxylic acid proton, however, will disrupt this hydrogen bonding and allow the reaction sequence to occur. Thus the reaction scheme [3] should be revised as follows:

Br = Bilirubin with a deprotonated carboxylic acid group.

and

Bv = Biliverdin with a deprotonated carboxylic acid group.

All species in the scheme should therefore bear an extra +1 formal charge. Proton loss as drawn then pertains to pyrrole or methine protons only.

Acknowledgement

We thank the Office of Naval Research, Washington, for support of part of this work.

References

1. A. W. Aylmer-Kelly, A. Bewick, P. R. Cantrell, and A. M. Tuxford, Disc Faraday Soc. 56 (1973) 96.

2. A. Bewick, J. Mellor, and S. Pons, Electrochim Acta 25 (1980) 931.

3. S. Pons and S. B. Khoo, J. Amer. Chem. Soc. 104 (1982) 3845.

4. A. Scott Hinman, Jerome F. McAleer, and Stanley Pons, J. Electroanal. Chem., in press.

5. D. E. Smith in A. J. Bard, Ed., "Electroanalytical Chemistry", Vol. 1, Marcel Dekker, N.Y., 1966 pp 1-155.

6. J. Fog, Scand. J. Clin. Lab. Invest. 16 (1964) 49.

7. P. Mannito and D. Monti, Specialia 35 (1979) 9.

8. H. Lund and P. Iversen in M. Baizer, Ed., "Organic Electrochemistry", Marcel Dekker, New York, 1973.

9. A. Scott Hinman and Stanley Pons, in preparation.

10. J. D. Van Norman and R. Szentirmay, Bioinorganic Chem. 4 (1974) 37.

11. C. H. Slifstein and M. Ariel, J. Electroanal. Chem. 48 (1973) 447.

12. ibid 75 (1976) 551.

13. J. D. van Norman and R. Szentirmay, Anal. Chem. 46 (1974) 1456.

14. T. R. Koch and O. O. Akingbe, Clin. Chem. 27 (1981) 1295.

15. J. F. McAleer, S. Pons, and J. Pradko, in preparation.

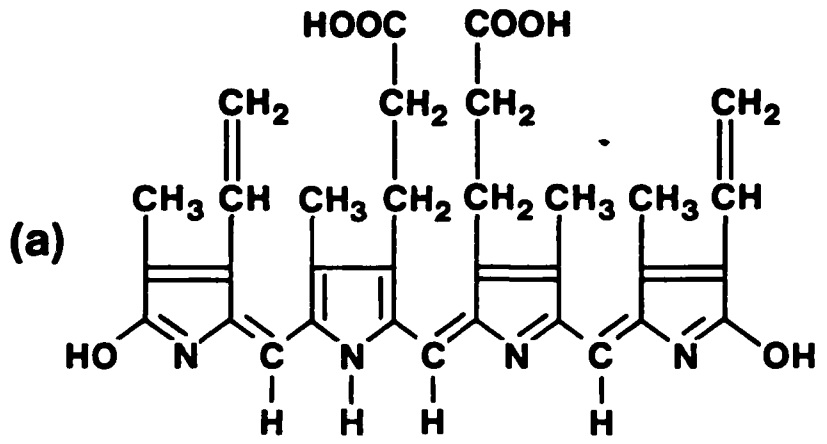

(a) Biliverdin IX — α

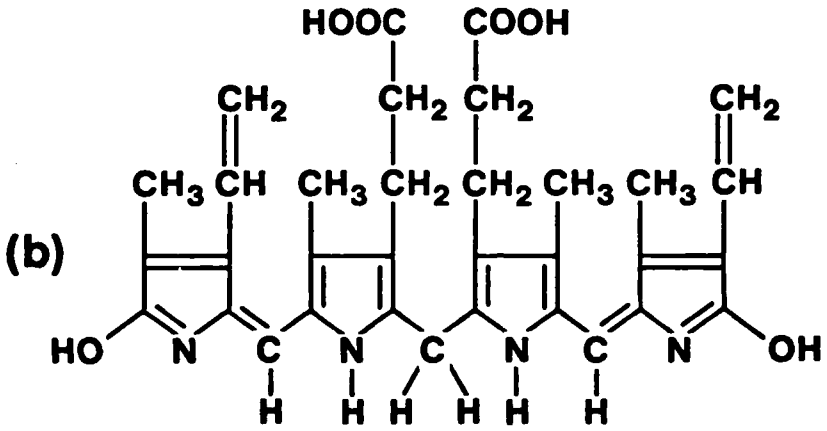

(b) Bilirubin IX — α

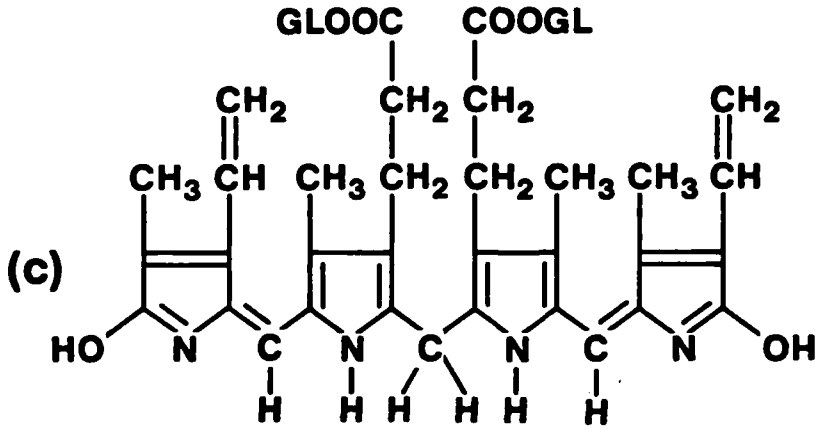

(c) Bilirubin IX — α diglucuronide

GL = glucuryl

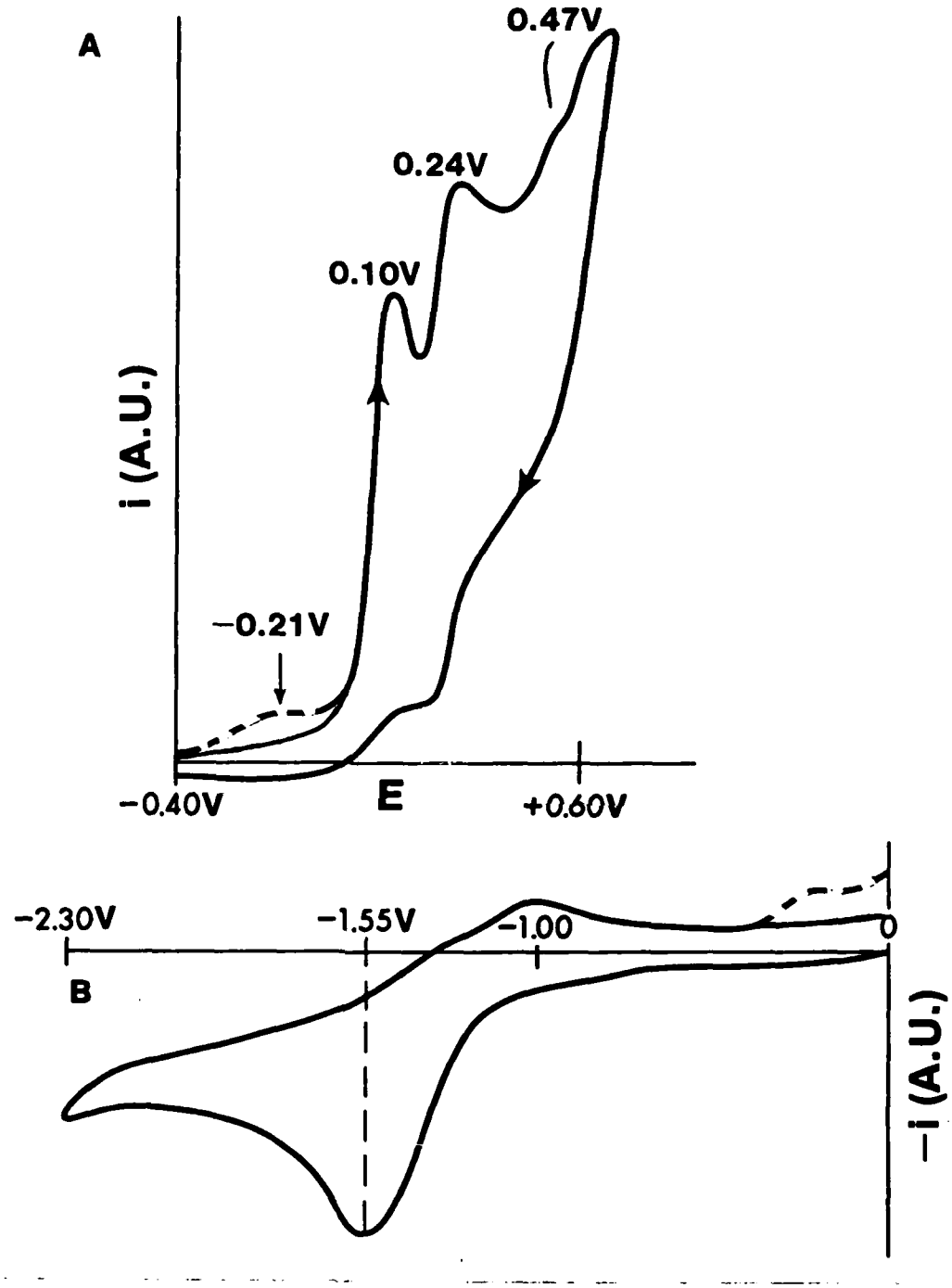
A
0.47V
0.24V
0.10V
i (A.U.)
−0.21V
−0.40V
E
+0.60V
−2.30V
−1.55V
−1.00
0
B
−i (A.U.)

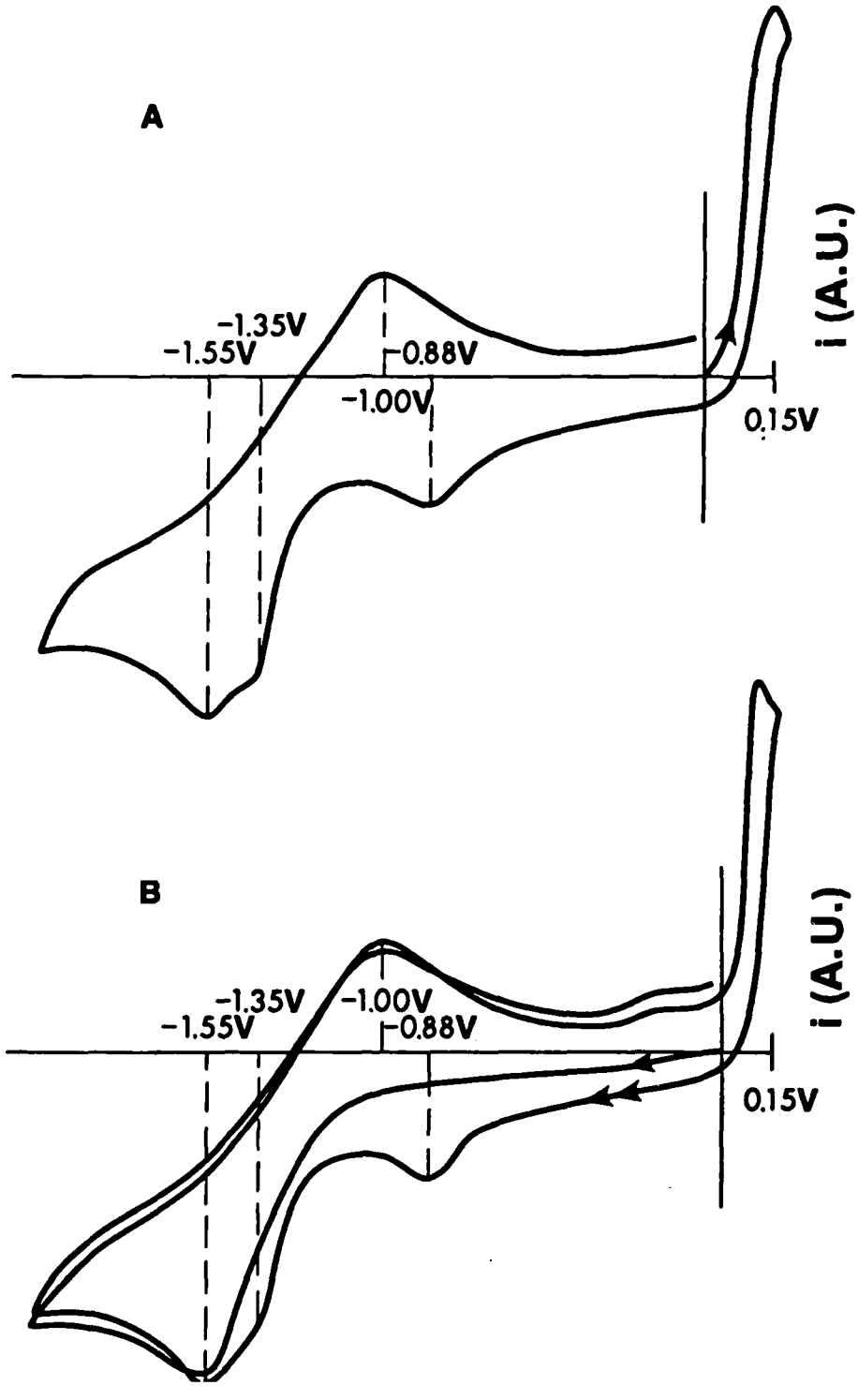
A
-1.35V
-1.55V
-0.88V
-1.00V
0.15V
i (A.U.)
B
-1.35V
-1.00V
-1.55V
-0.88V
0.15V
i (A.U.)

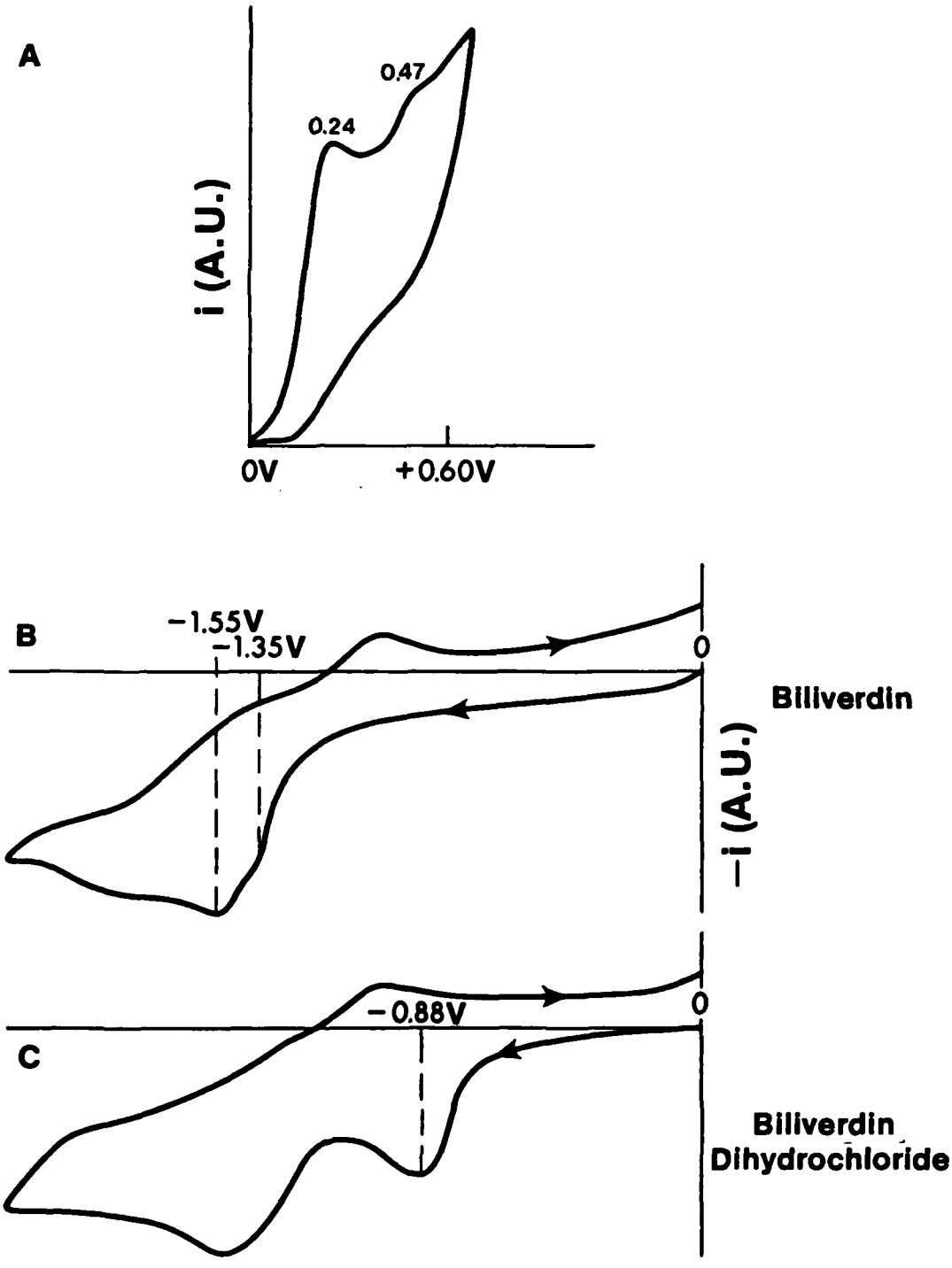
A
0.47
0.24
i (A.U.)
0V
+0.60V
B
−1.55V
−1.35V
0
Biliverdin
−i (A.U.)
−0.88V
0
C
Biliverdin
Dihydrochloride

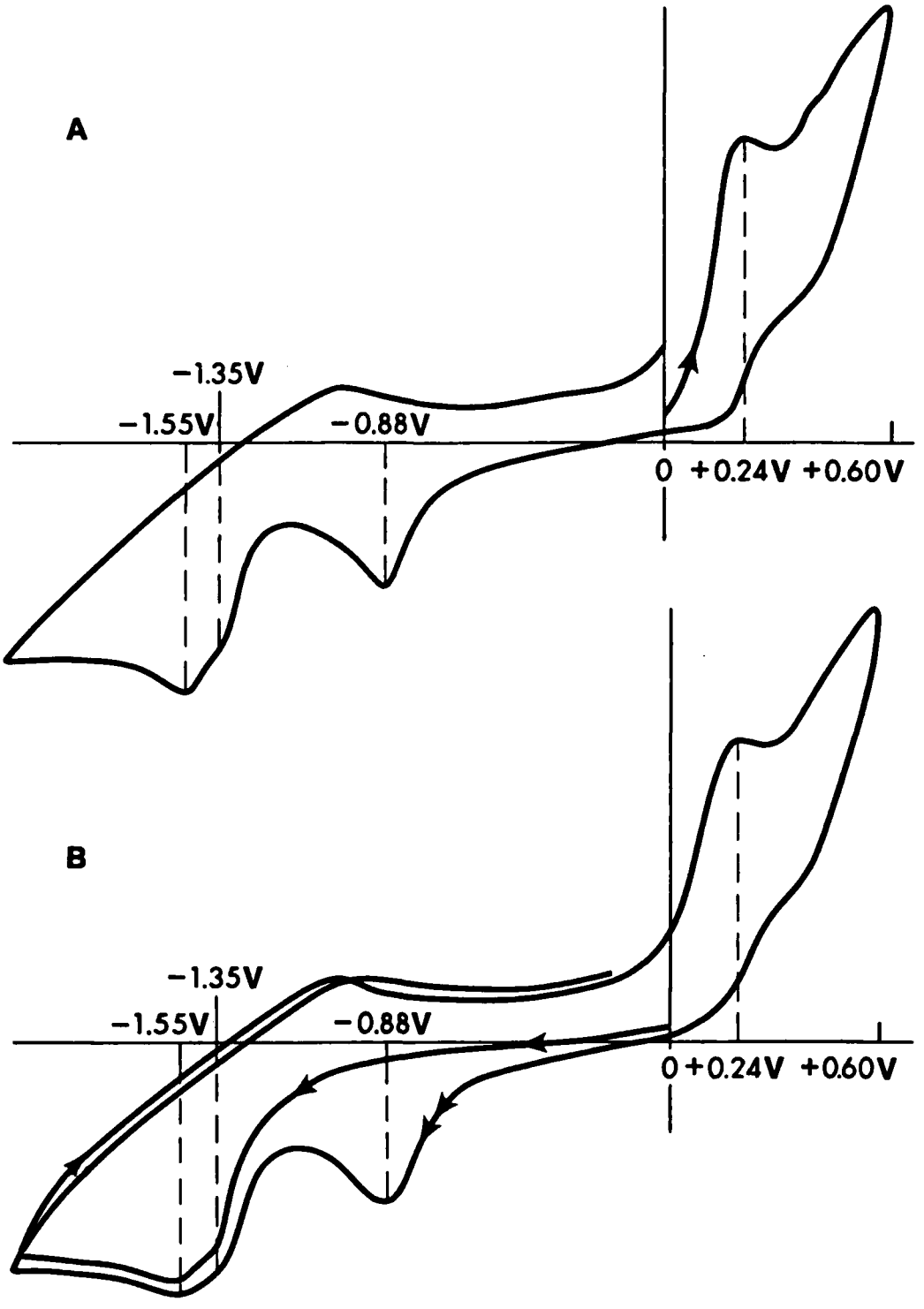
A
−1.35V
−1.55V
−0.88V
0
+0.24V
+0.60V
B
−1.35V
−1.55V
−0.88V
0
+0.24V
+0.60V

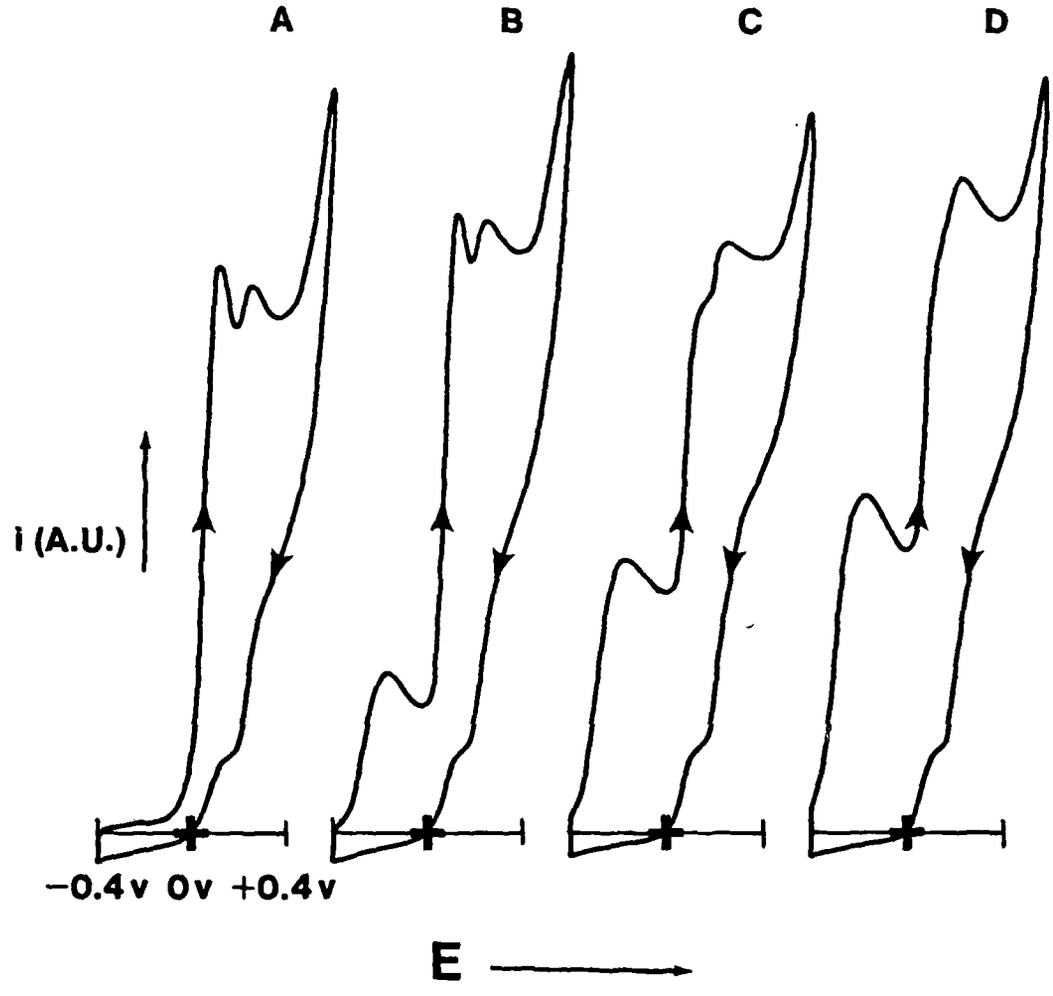
A
B
C
D
I (A.U.)
−0.4v 0v +0.4v
E

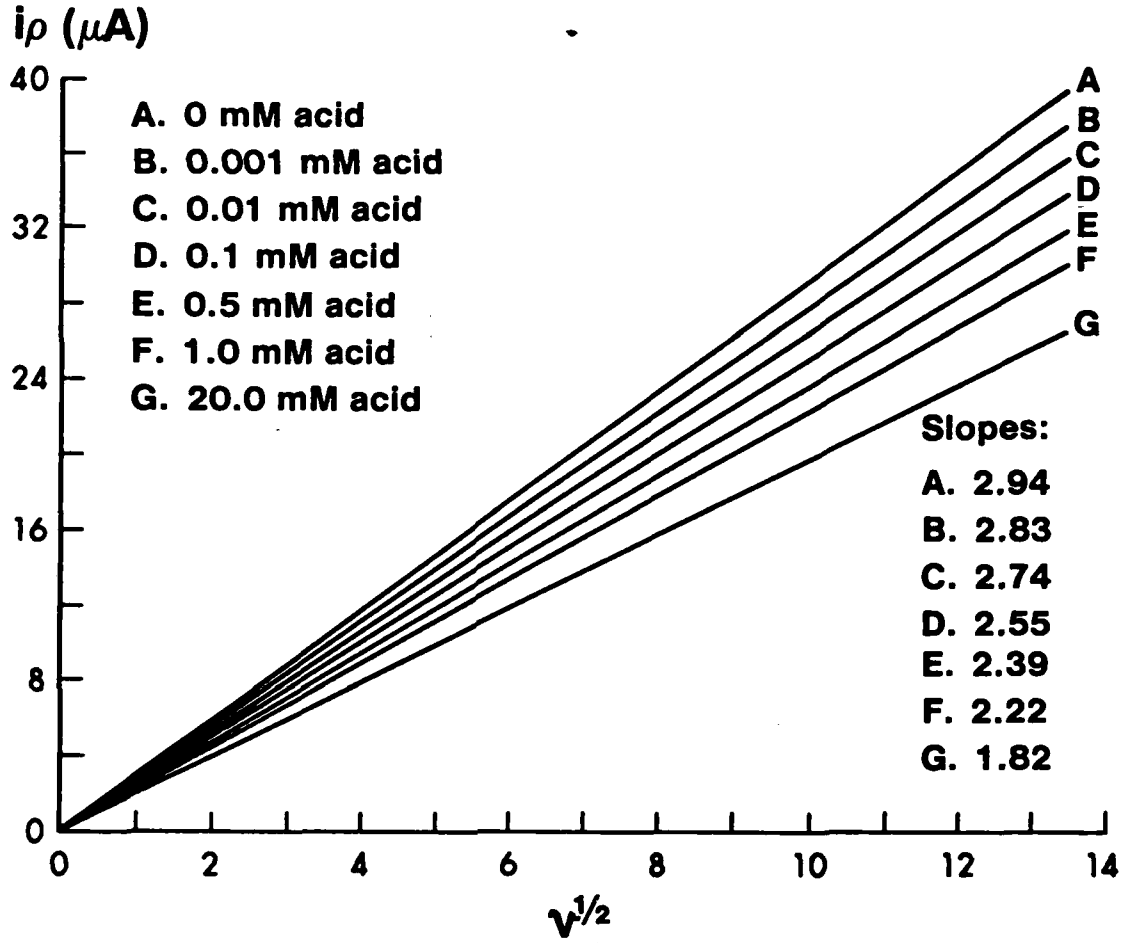
ip (μA)
40
32
24
16
8
0
A. 0 mM acid
B. 0.001 mM acid
C. 0.01 mM acid
D. 0.1 mM acid
E. 0.5 mM acid
F. 1.0 mM acid
G. 20.0 mM acid
A
B
C
D
E
F
G
Slopes:
A. 2.94
B. 2.83
C. 2.74
D. 2.55
E. 2.39
F. 2.22
G. 1.82
0
2
4
6
8
10
12
14
V1/2

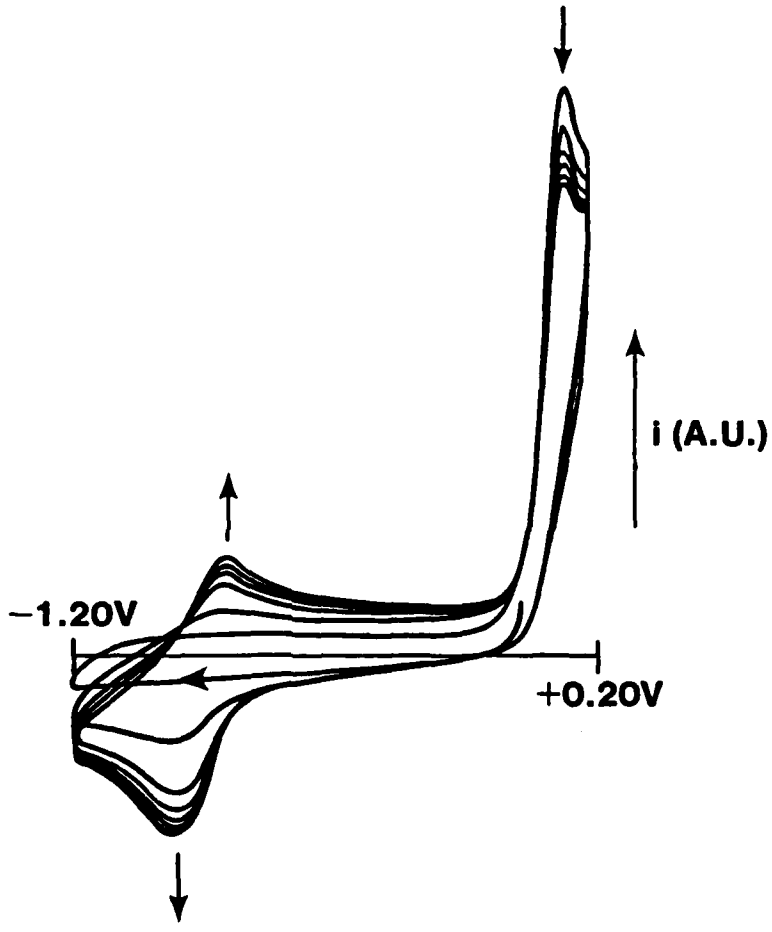
i (A.U.)
−1.20V
+0.20V

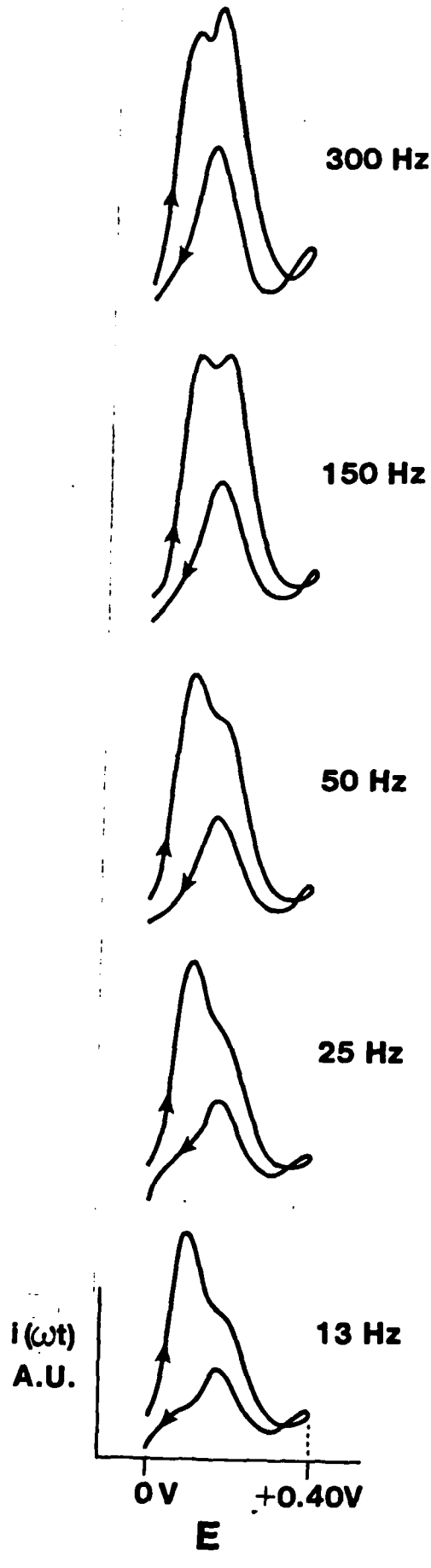
300 Hz
150 Hz
50 Hz
25 Hz
13 Hz
I(ωt)
A.U.
0 V
+0.40V
E

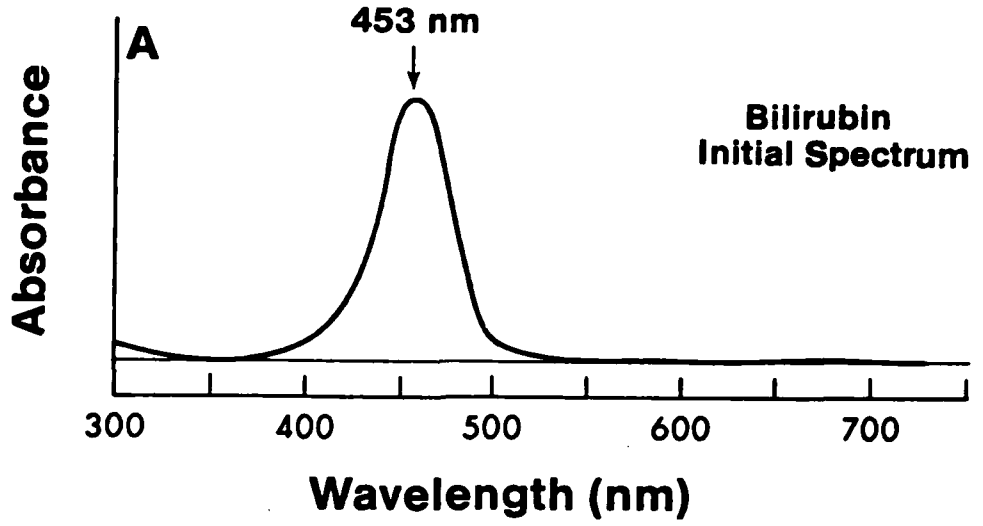
A
453 nm
Bilirubin
Initial Spectrum
Absorbance
300
400
500
600
700
Wavelength (nm)

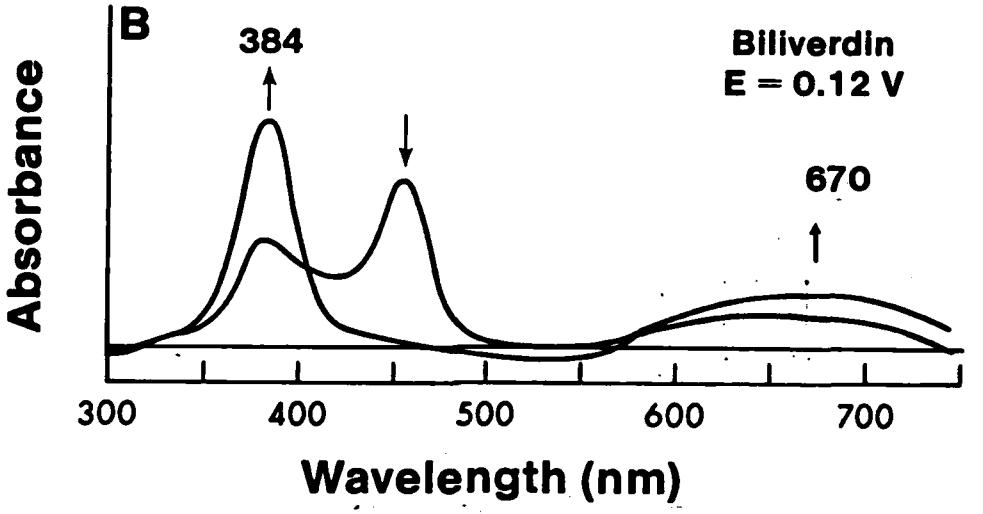
B
384
Biliverdin
E = 0.12 V
670
Absorbance
300
400
500
600
700
Wavelength (nm)

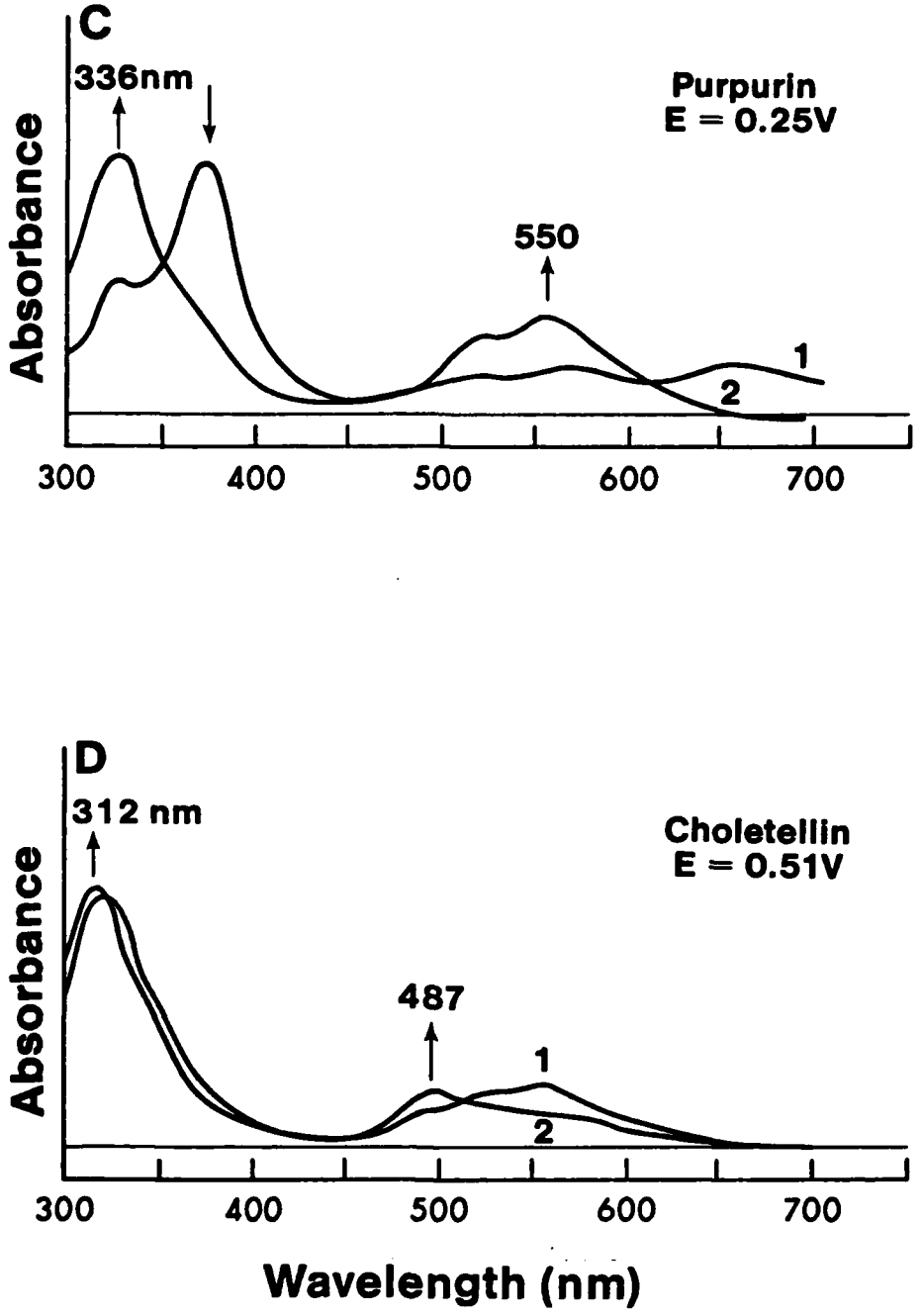
C
336nm
Purpurin
E = 0.25V
550
1
2
Absorbance
300
400
500
600
700
D
312 nm
Cholетellin
E = 0.51V
487
1
2
Absorbance
300
400
500
600
700
Wavelength (nm)

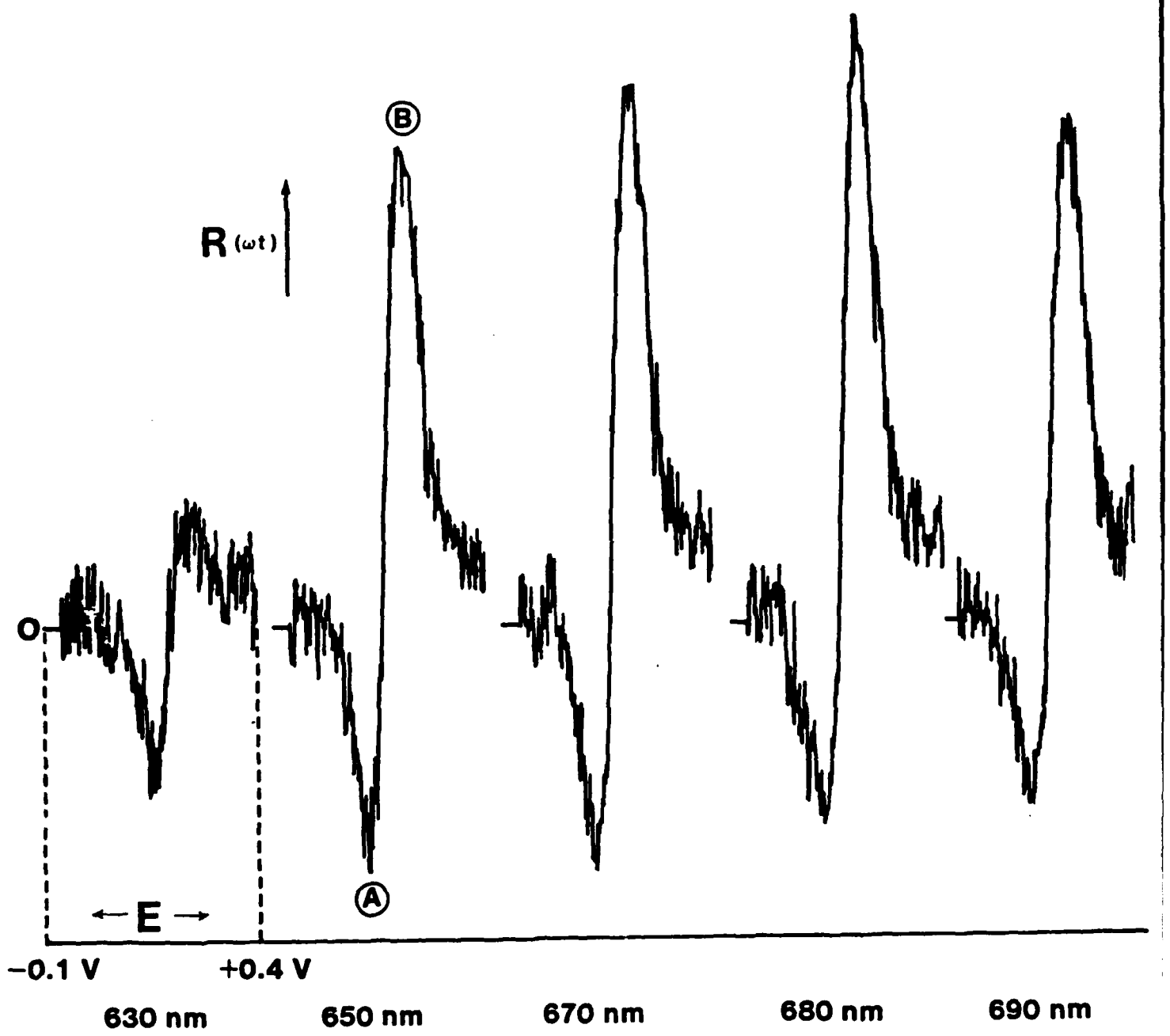
B
R (ωt)
O
A
← E →
−0.1 V
+0.4 V
630 nm
650 nm
670 nm
680 nm
690 nm

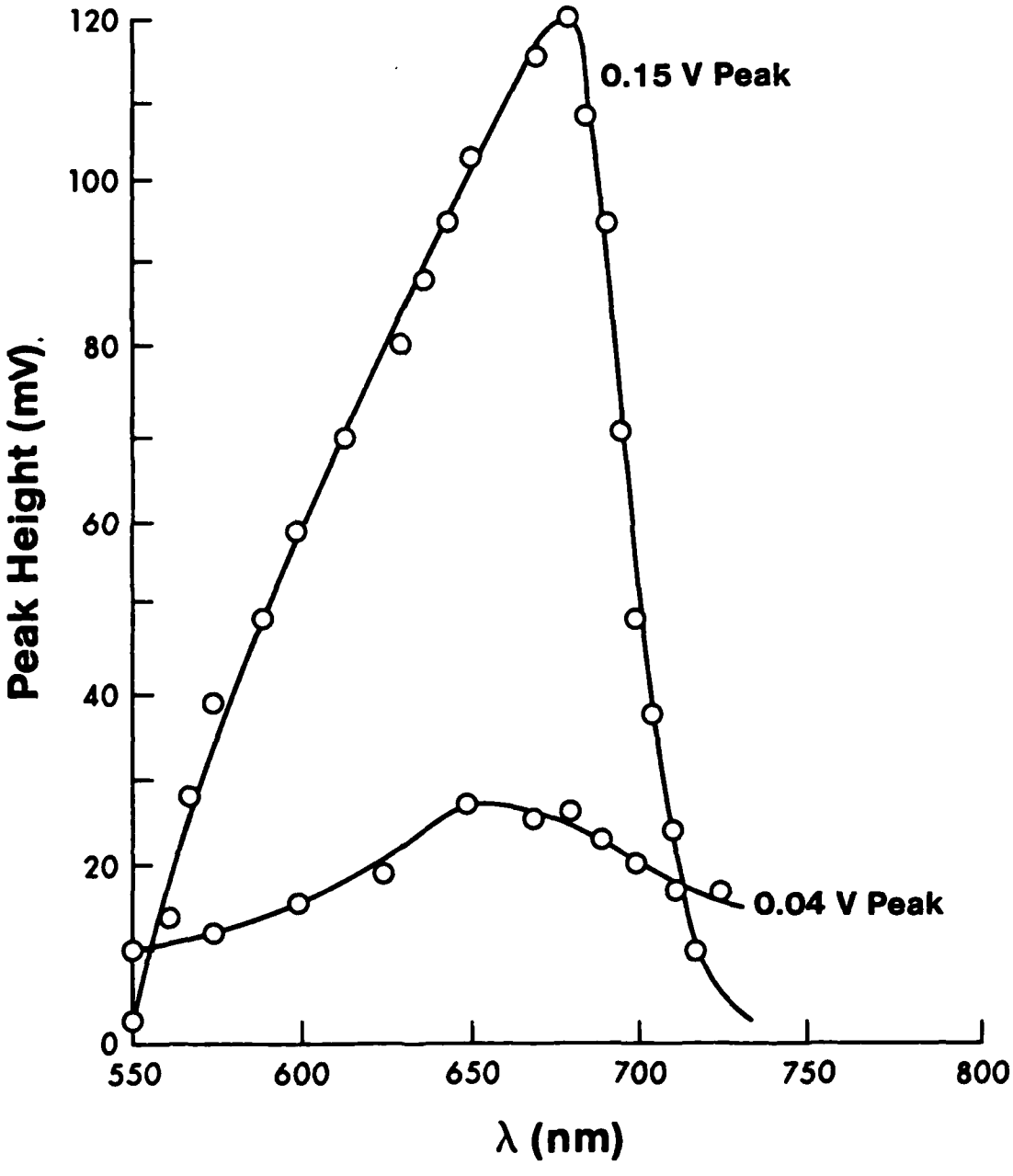
120
100
80
60
40
20
0
Peak Height (mV)
0.15 V Peak
0.04 V Peak
550
600
650
700
750
800
λ (nm)

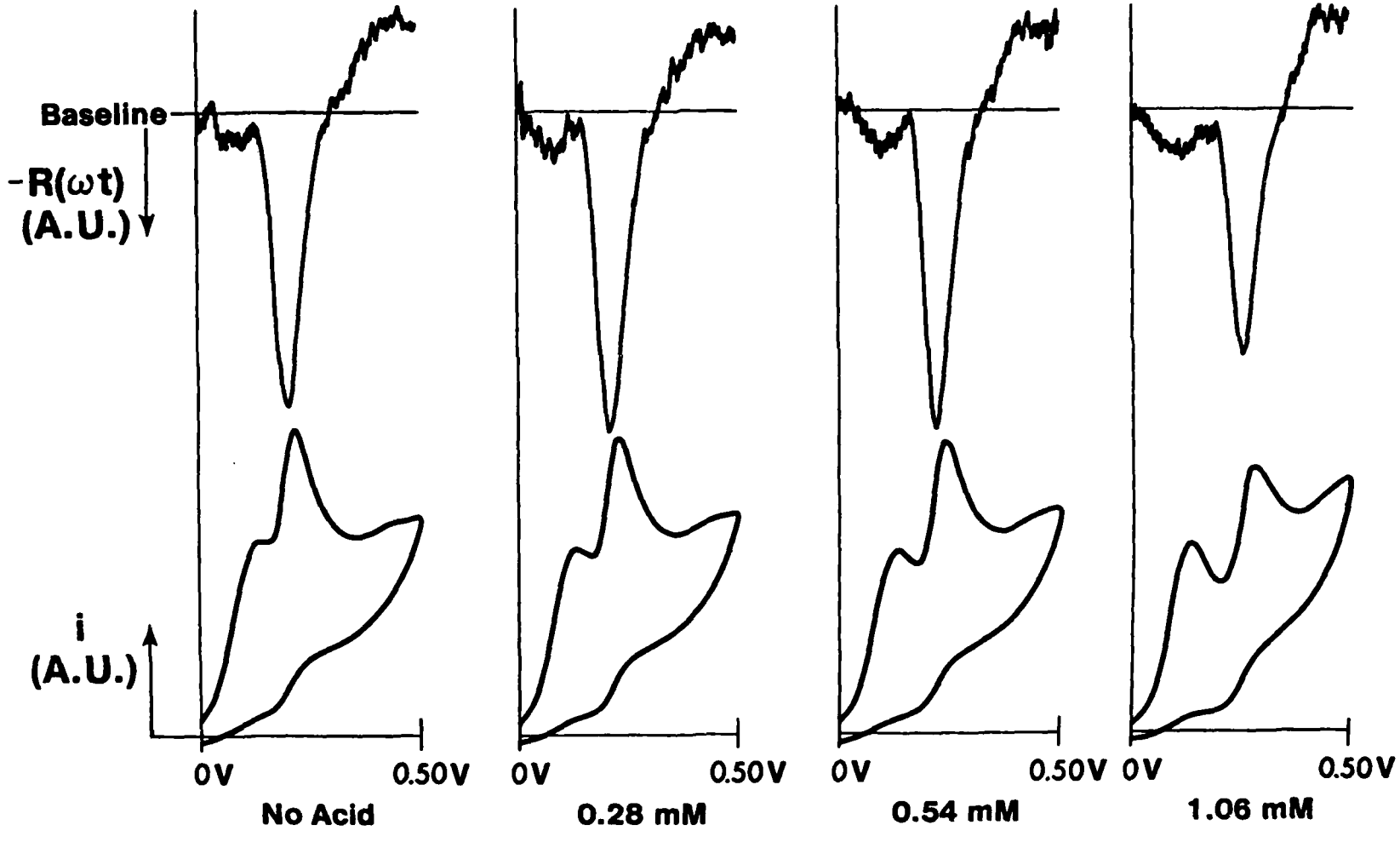
Baseline
-R(ωt)
(A.U.)
i
(A.U.)
0V
0.50V
No Acid
0.28 mM
0.54 mM
1.06 mM

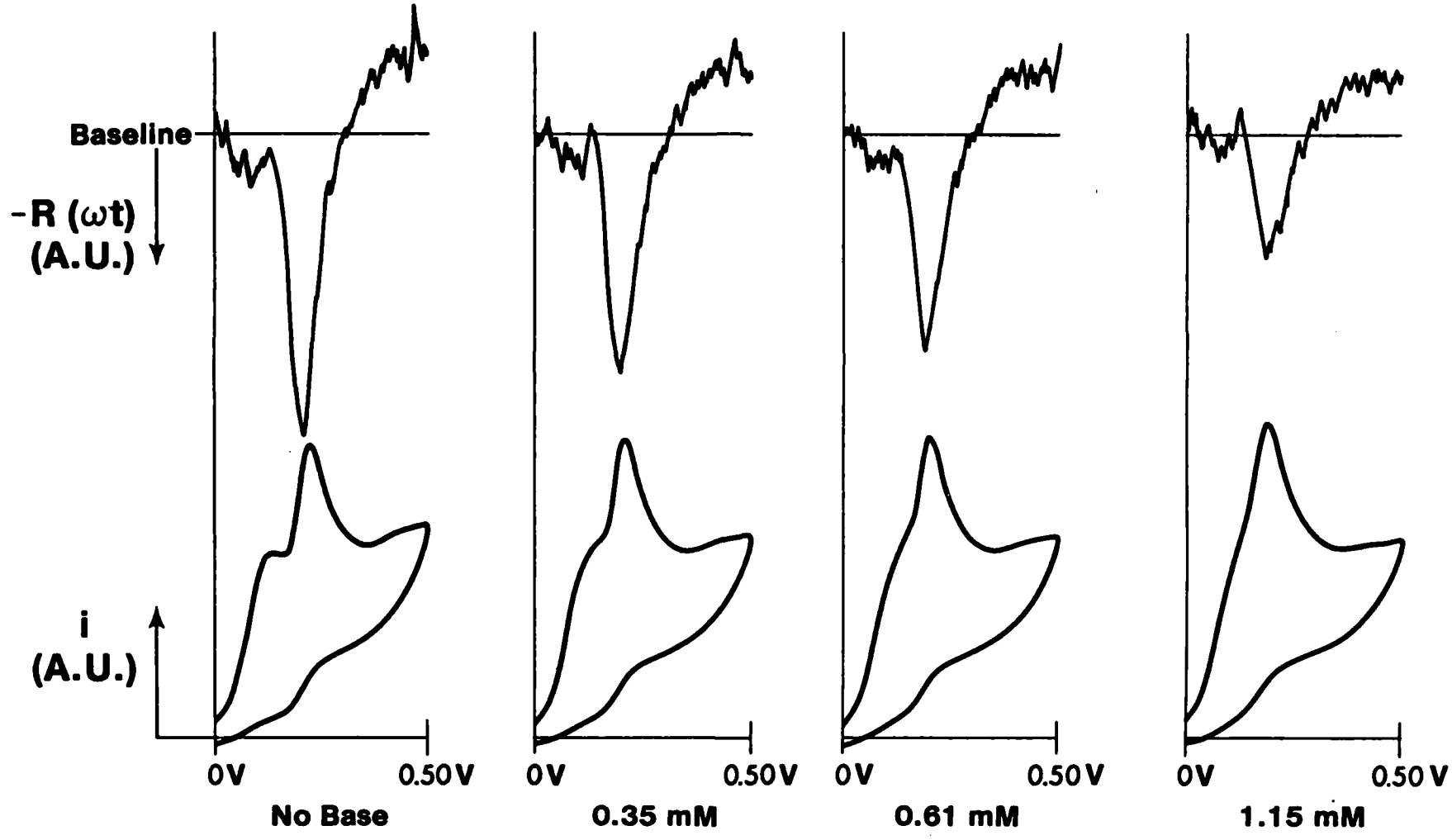
Baseline
-R (ωt)
(A.U.)
i
(A.U.)
0V
0.50V
No Base
0V
0.50V
0.35 mM
0V
0.50V
0.61 mM
0V
0.50V
1.15 mM

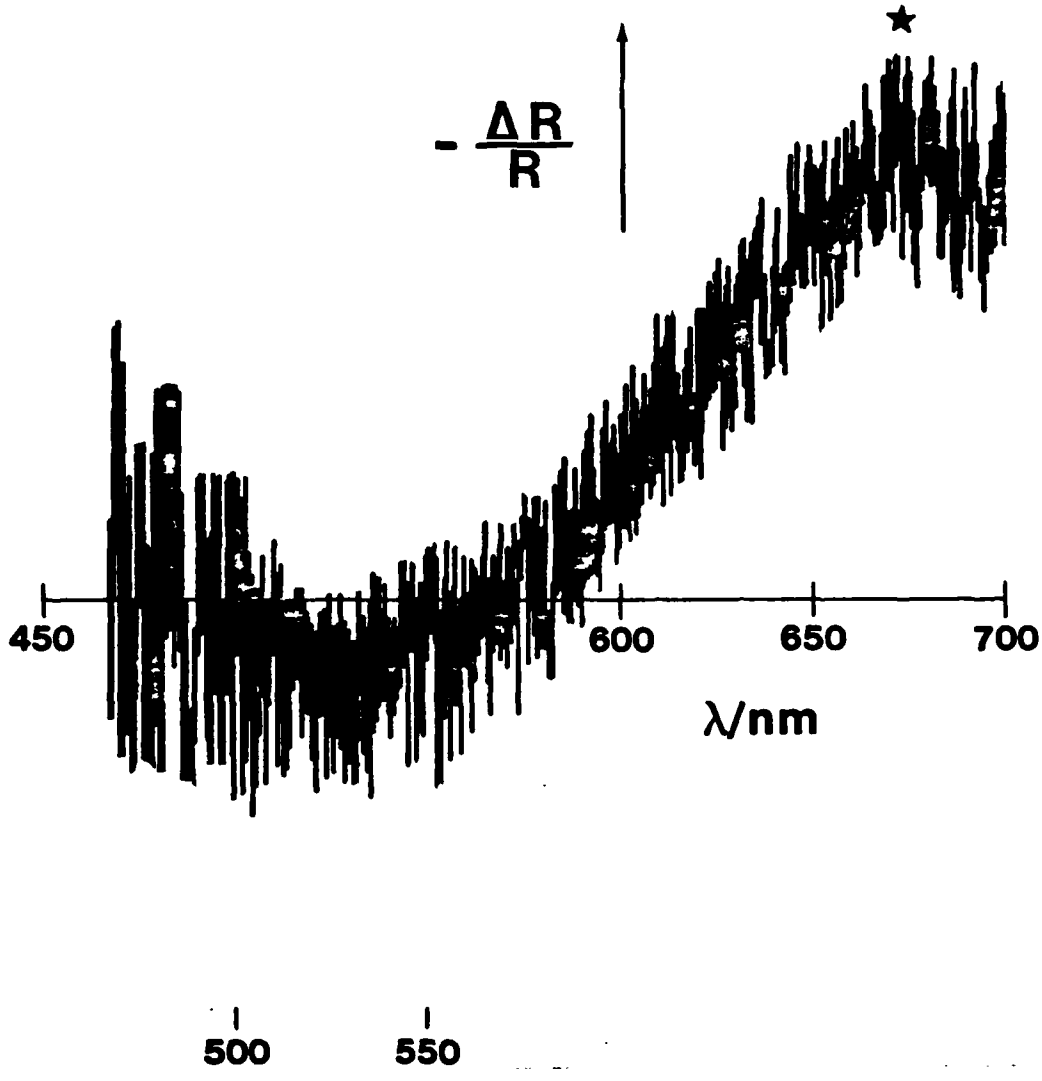
- ΔR/R
450
600
650
700
λ/nm
500
550

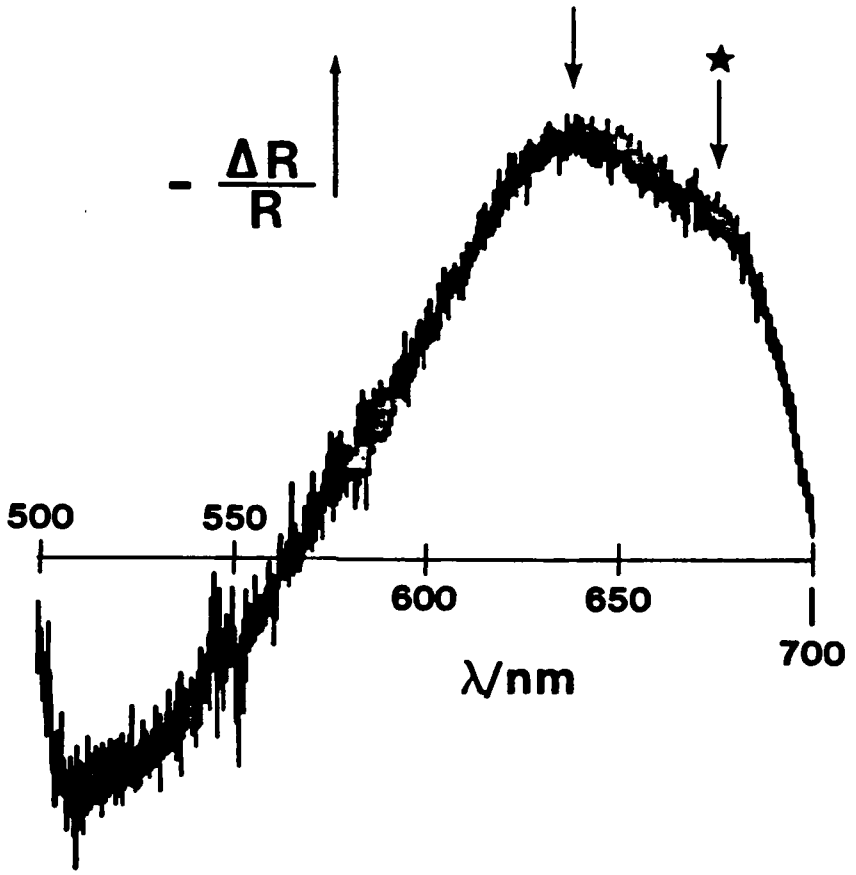
- ΔR/R
500
550
600
650
700
λ/nm

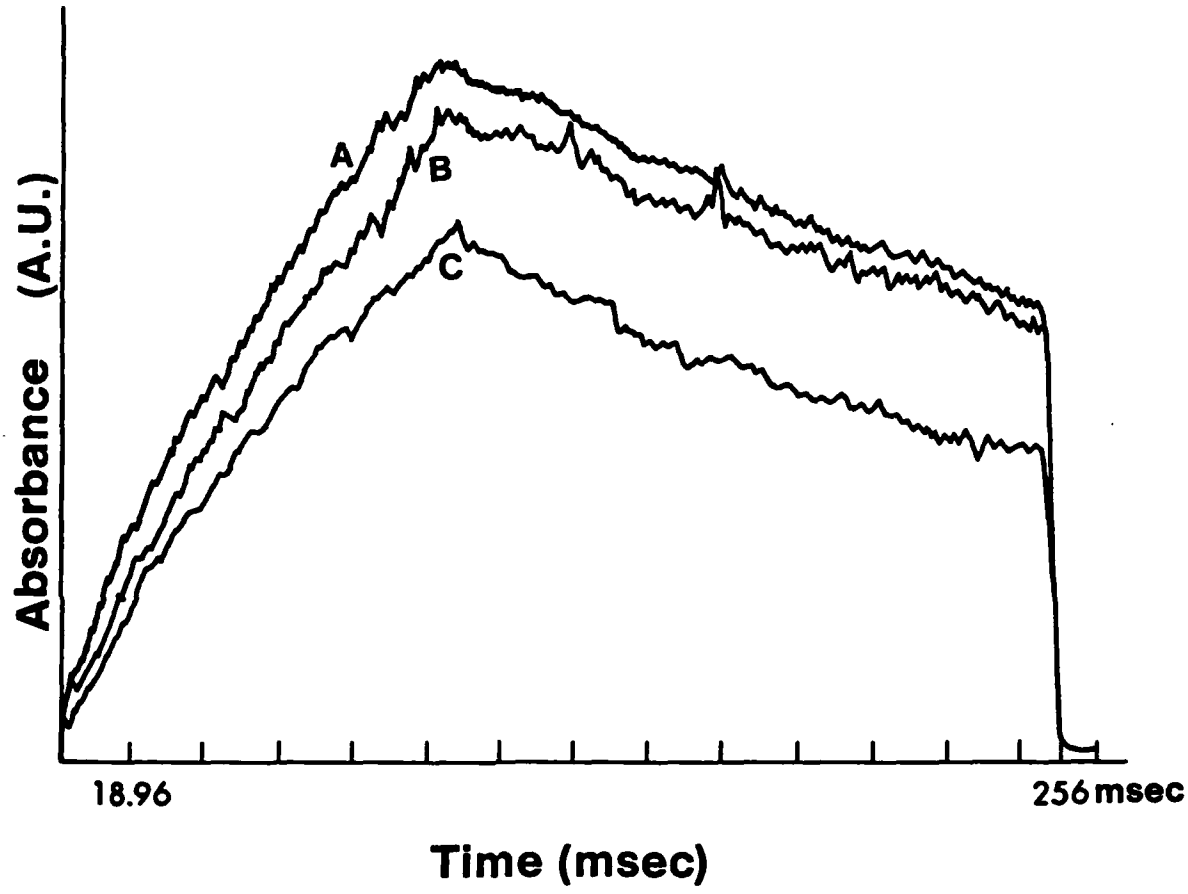
Absorbance (A.U.)
A
B
C
18.96
256 msec
Time (msec)

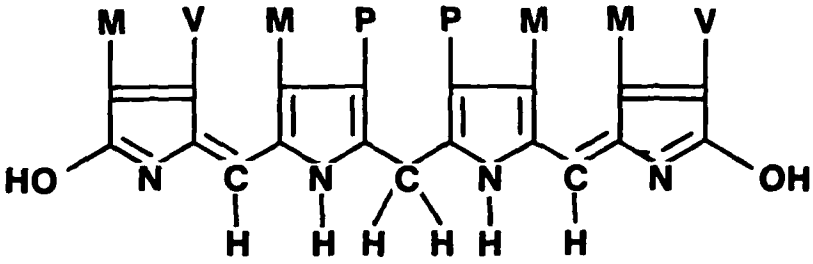

Bilirubin **Yellow**
biladiene a,c

$-2e^-$

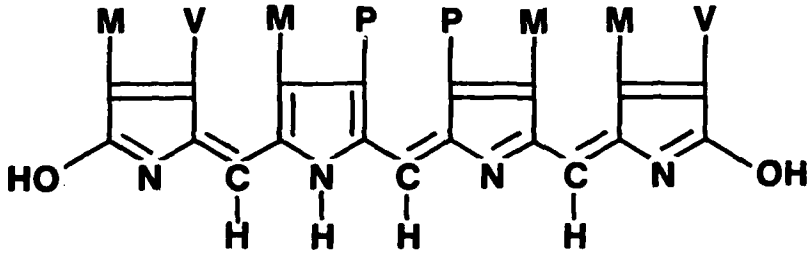

Biliverdin **Green**
bilatriene

$-2e^-$

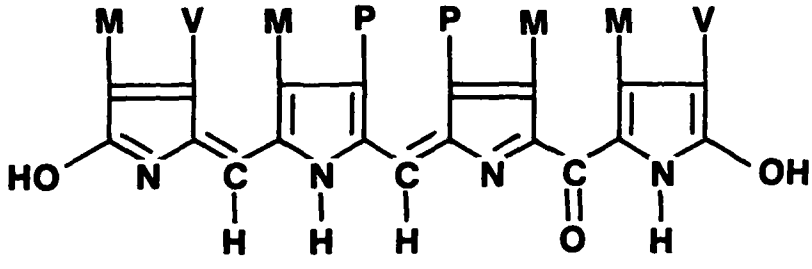

Purpurin **Purple**
biladiene -a,b-one-c

$-2e^-$

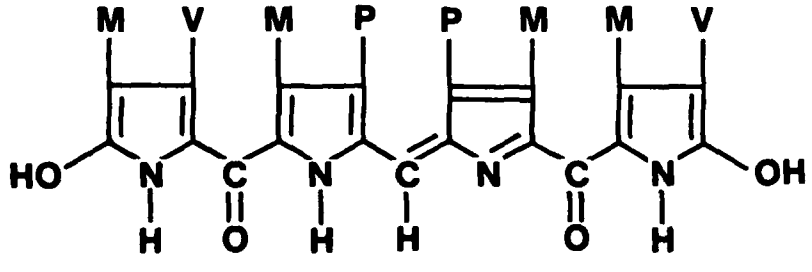

Choletellin **Yellow**
biladiene -b-one-a,c

END

FILMED

1-85

DTIC